DOI: 10.1002/ejic.201000252

γ-Deprotonation of Bridging Vinyliminium Ligands: New Route to Aminobutadienylidene Diiron and Diruthenium Complexes

Luigi Busetto,[a] Fabio Marchetti,[b][‡] Mauro Salmi,[a] Stefano Zacchini,[a] and Valerio Zanotti*[a]

Keywords: Vinylidene ligands / Deprotonation / Iron / Ruthenium / Dinuclear complexes

The SPh-functionalized vinyliminium complexes $[M_2\{\mu\text{-}\eta^1{:}\eta^3\text{-}C(R')=C(SPh)C=N(Me)(R)\}(\mu\text{-}CO)(CO)(Cp)_2][SO_3CF_3]$ [M = Fe, R = Xyl, R′ = Me, **2a**; M = Fe, R = Me, R′ = Me, **2b**; M = Fe, R = 4-C_6H_4OMe, R′ = Me, **2c**; M = Ru, R = Xyl, R′ = Me, **2d**; M = Fe, R = Xyl, R′ = CH_2OH, **2e**; M = Fe, R = Me, R′ = CH_2OH, **2f**; Xyl = 2,6-$Me_2C_6H_3$] react upon treatment with NaH in thf solution. Species **2a** and **2c** afford the dinuclear butadienylidene complexes $[Fe_2\{\mu\text{-}\eta^1{:}\eta^3\text{-}CN(R)(Me)=C(SPh)C=CH_2\}(\mu\text{-}CO)(CO)(Cp)_2]$ (R = Xyl, **4**; R = 4-C_6H_4OMe, **8**), respectively. The transformation of **2c** into **8** is selective, whereas **2a** produces **4** together with the metallacycle [Fe(CO)(Cp){CN(Xyl)(Me)C(SPh)C(Me)C(O)}] (**3**). A very similar metallacycle [Fe(CO)(Cp){$CN(Me)_2C(SPh)$-C(Me)C(O)}] (**7**) is obtained, as a single product, from **2b**. Diruthenium complex **2d**, upon treatment with NaH, affords the dinuclear butadienylidene complex $[Ru_2\{\mu\text{-}\eta^2{:}\eta^3\text{-}CN(Me)(Xyl)=C(SPh)C=CH_2\}(CO)_2(Cp)_2]$ (**9**), which is very similar to diiron species **4** and **8**, but it exhibits a different bridging coordination mode, as evidenced by X-ray diffraction. Complexes **2d** and **2f** upon treatment with NaH undergo deprotonation of the OH group, which consequently gives rise to an intramolecular nucleophilic addition to the CO group to yield the complexes $[Fe_2\{\mu\text{-}\eta^1{:}\eta^3\text{-}C\{CH_2OC(O)\}=C(SPh)C=N(Me)(R)\}(\mu\text{-}CO)(Cp)_2]$ (R = Xyl, **10a**; R = Me, **10b**). This transformation is reversed upon treatment with HSO_3CF_3. The molecular structures of **8**, **9**, and **10a**·$0.33CH_2Cl_2$·were determined by X ray diffraction studies.

Introduction

Multiside bound organic frames are expected to show a reactivity different from that observed when the same molecules are noncoordinated or are bound to a single metal center.[1] This is also the case for diiron vinyliminium complexes **1**[2] (Scheme 1), in which the bridging ligand undergoes transformations that are unusual for noncoordinated α,β-unsaturated iminium species.[3] As an example, μ-vinyliminium ligands undergo nucleophilic addition at the iminium carbon atom or at the adjacent α-C in place of the expected Michael-type conjugate addition (addition at the β position).[4]

A further reaction involving vinyliminium complexes that is uncommon in noncoordinated α,β-unsaturated iminium ions is α-deprotonation and subsequent α-functionalization. Indeed, proton removal from the α position in iminium compounds generates enamines, which can react with electrophiles to give α-modified iminium ions.[5] Enamines are powerful tools in organic synthesis and fundamental intermediates in enamine catalysis (amino catalysis).[6] On the other hand, conjugated iminium ions do not undergo α-deprotonation, but rather they act as Michael acceptors.[3] Combination of the iminium and enamine reaction modes into one mechanism has led to the development of organocascade catalysis, which is a rapidly expanding synthetic approach.[7] In the light of these considerations, the reactivity of α,β-unsaturated iminium ions as bridging ligands appears unique in that they undergo α C-H abstraction upon treatment with NaH, leading to the formation of reactive intermediates.[8] These can be combined with a variety of reagents, (e.g., elemental sulfur or selenium,[9] diazoacetates,[10] arylisocyanides,[11] and phenyldisulfides[12]), re-

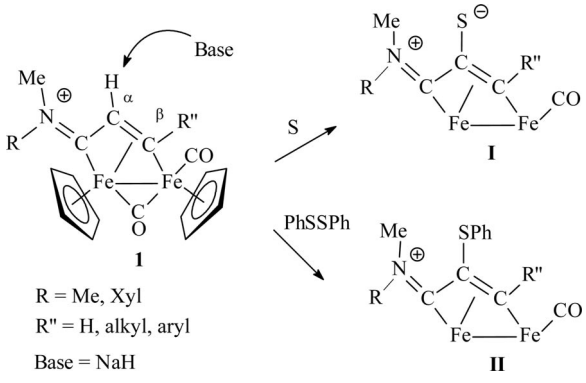

Scheme 1. μ-CO and Cp ligands are omitted for clarity in products **I** and **II**.

[a] Dipartimento di Chimica Fisica e Inorganica, Università di Bologna,
Viale Risorgimento 4, 40136 Bologna, Italy
[b] Dipartimento di Chimica e Chimica Industriale, Università di Pisa,
via Risorgimento 35, 56126 Pisa, Italy
E-mail: valerio.zanotti@unibo.it
[‡] Fabio Marchetti, born in 1974 in Bologna, Italy

WILEY InterScience DISCOVER SOMETHING GREAT
© 2010 Wiley-VCH Verlag GmbH & Co. KGaA, Weinheim

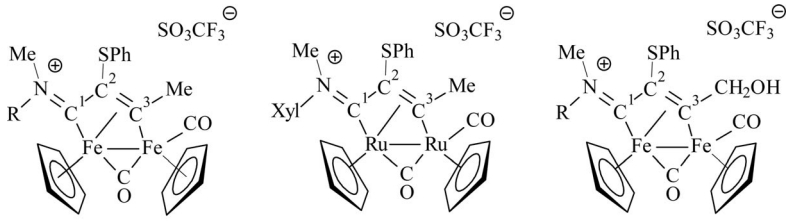

2a R = Xyl (Xyl =2,6-$Me_2C_6H_3$)
2b R = Me
2c R = 4-C_6H_4OMe
2d
2e R = Xyl
2f R = Me

Scheme 2.

sulting in the replacement of the α C-H with a range of functional groups (α-functionalization). As an example, some of the complexes obtained by replacing the C–H with C–S bonds are shown in Scheme 1.

In the course of these investigations it was found that there was some variability in the yield of complexes of type **II**, suggesting that the products were themselves reactive toward NaH. In the absence of the acidic α-CH hydrogen, deprotonation might have occurred at other sites of the bridging iminium ligand.

The present report concerns a more detailed study on the γ-deprotonation of bridging phenylthiolate vinyliminium diiron and diruthenium complexes **2a**–**d** shown in Scheme 2 and the consequent formation of bridging ligands displaying aminobutadienyl character.

Results and Discussion

SPh-functionalized vinyliminium complex **2a** reacts in the presence of a large excess of NaH in thf solution to afford a mixture of two products: metallacyclopentadienone **3** and aminobutadienylidene diiron complex **4**, obtained in about 65 and 20% yield, respectively (Scheme 3).

Compounds **3** and **4** were separated by column chromatography and characterized by spectroscopic methods and elemental analysis. In Schemes 2 and 3 the carbon atoms of the bridging chain have been labeled so that the discussion and the considerations presented hereafter are clear. Compound **3** closely resembles metallacyclopentadienone complex **5** (Scheme 4), which was previously obtained by a similar procedure consisting in the treatment of the vinyliminum complex $[Fe_2\{\mu\text{-}\eta^1\text{:}\eta^3\text{-}CN(Xyl)(Me)CHCMe\}(\mu\text{-}CO)(CO)(Cp)_2][SO_3CF_3]$ (**1a**) with NaH.[8] The two metallacyclopentadienone complexes differ only in the nature of the C^2-hexocyclic substituent, which is SPh in **3** and H in **5**. As for the synthesis of **5**, the fragmentation of the parent diiron compound is presumably favored by the reducing conditions, and the metallacycle results from assembly of the bridging C_3 fragment with a CO ligand.

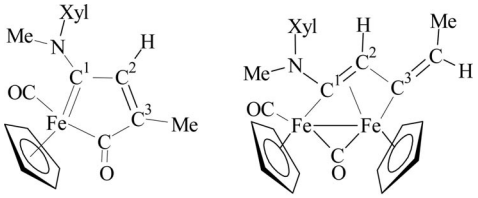

5 **6**

Scheme 4.

On the other hand, compound **4** resembles the μ-butadienylidene complex $[Fe_2\{\mu\text{-}\eta^1\text{:}\eta^3\text{-}C(Ph)C(Ph)C{=}CH_2\}(\mu\text{-}CO)(CO)(Cp)_2]$,[13] which exhibits an analogous bridging C_4 ligand, except for the fact that it does not contain heteroatoms. A closer analogy is complex **6** (Scheme 4), which was obtained by coupling of the allene $CH_2{=}C{=}CHMe$ with the aminocarbyne complex $[Fe_2\{\mu\text{-}CN(Me)(R)\}(\mu\text{-}CO)(CO)_2(Cp)_2][SO_3CF_3]$.[14]

The spectroscopic properties of **3** and **4** are obviously similar to those of **5** and **6**. The IR spectrum (in CH_2Cl_2 solution) of **3** shows two νCO absorptions at 1922 and 1582 cm^{-1} due to the CO ligand and the acyl group, respectively. In the ^{13}C NMR spectra of **3**, typical low-field resonances were found for the acyl carbon atom (δ = 267.9 ppm) and for the C^1 carbon atom (δ = 271.8 ppm), which exhibits some aminocarbene character.

Concerning **4**, the ^{13}C NMR spectroscopic data are consistent with the butadienylidene nature of the bridging ligand. The C^1, C^2, and C^3 resonances are observed at 200.3

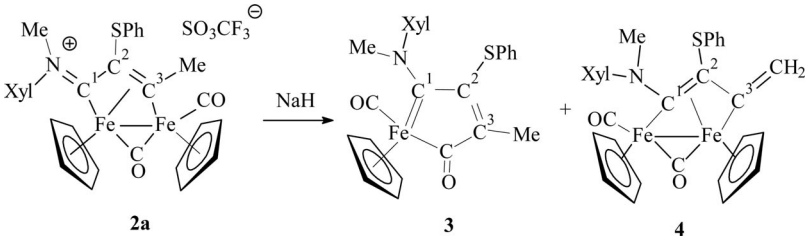

2a **3** **4**

Scheme 3.

 © 2010 Wiley-VCH Verlag GmbH & Co. KGaA, Weinheim

82.2, and 178.3 ppm, respectively, whereas the signal due to the CH_2 termination occurs at δ = 102.4 ppm.

The formation of butadienylidene complex **4** merits further comment. For the first time, we observed deprotonation of the vinyliminium ligand at the C^3-CH_3 substituent (γ position). This corresponds to γ-deprotonation of an α,β-unsaturated iminium ion, leading to the formation of the corresponding dienamine (Scheme 5). Despite being a well-known possibility, the formation of dienamines by deprotonation of conjugated iminium ions has so far been underexploited.[15] Likewise, the synthetic potential of dienamine catalysis for the γ-activation of α,β-unsaturated aldehydes has been investigated only to a limited extent.[16] Our results evidence that γ-deprotonation can be assisted by bridging coordination, as the diiron frame provides stability to the dienamine (aminobutadienylidene) ligand consequently generated. It should be noted that a change in the coordination mode takes place along with the transformation of **2a** into **4**: a terminally coordinated CO ligand shifts from one Fe atom to the other, which is made possible by the rather flexible nature of the diiron frame.

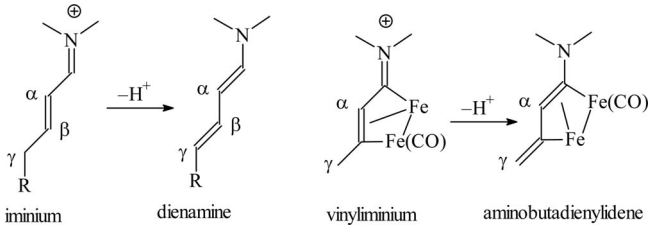

Scheme 5. General scheme for γ-deprotonation.

A further consideration concerns the very different nature of complexes **3** and **4**, which suggests the existence of two parallel mechanisms operating in the reaction of **2a** with NaH. The formation of butadienylidene **4** is clearly the result of γ-deprotonation, whereas metallacycle **3** contains the intact parent bridging C_3 frame, without any proton loss. In this case, NaH presumably acts as a reducing agent rather than as a base, supporting the fragmentation of the dinuclear unit. To investigate this point, compound **2a** was treated with sodium naphthalide (NaNaph) in the place of NaH to favor reduction instead of deprotonation. The reaction produced metallacycle **3** as the unique product, which is consistent with the hypothesis of a mechanism based on the reduction of the dinuclear parent complex. On the other hand, treatment of **2a** with KO*t*Bu yielded selectively butadienylidene **4**, without any detectable amount of metallacycle **3**.

In consideration of the fact that the reactivity of bridging vinyliminium ligands is largely influenced by the nature of the substituents (particularly of those on the N atom),[4] investigations were extended to vinyliminium complexes **2b** and **2c** containing methyl and methoxyphenyl groups, respectively, in the place of the Xyl group. The corresponding reactions with NaH afforded products similar to those described for the reaction of **2a**, except that the reactions are more selective. Both **2b** and **2c** yield one single product. Indeed, **2b** exclusively produces metallacyclopentadienone **7**, whereas **2c** leads to the formation of diiron complex **8**, analogous to **4** (Scheme 6).

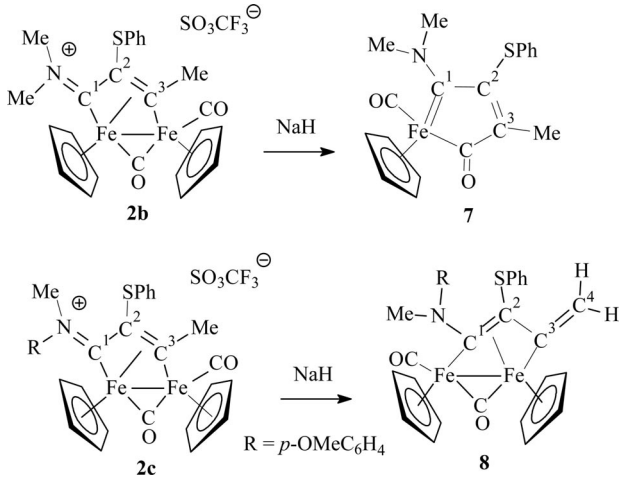

Scheme 6.

The reason for the different behavior of **2b** and **2c** is not obvious, although it must be related to the nature of the N substituents. Compounds **7** and **8** were characterized by spectroscopic methods and elemental analysis. Moreover, the X-ray structure of **8** was determined (Figure 1 and Table 1). The bonding parameters of **8** are compared to those of **6** in Table 1, indicating a very close similarity between the bridging ligands present in the two species. In particular, the coordination of the bridging unsaturated C_4 fragment to the diiron core exhibits high delocalization, which can be explained by using three different representation forms: the bridging allylidene (**A**), the aminoallenylalkylidene (**B**), and the 1-amino-1,3-butadienylidene (**C**; Scheme 7).

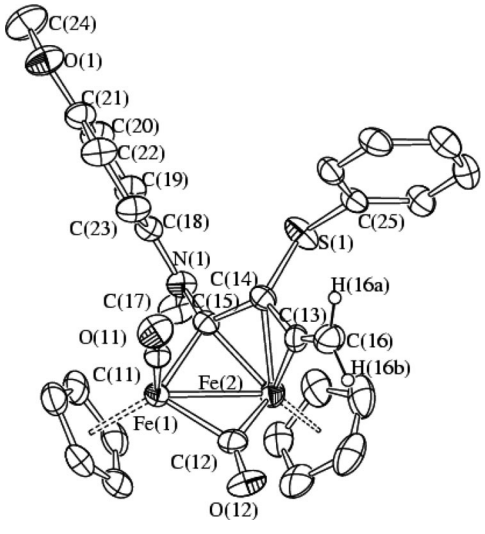

Figure 1. Molecular structure of **8** with key atoms labeled [all H atoms except for H(16a) and H(16b) are omitted for clarity]. Thermal ellipsoids are at the 30% probability level. Only one of the two independent molecules present in the unit cell is drawn.

 © 2010 Wiley-VCH Verlag GmbH & Co. KGaA, Weinheim

Table 1. Selected bond lengths [Å] and angles [°] for **8** (data for both the independent molecules present within the unit cell are reported); data of **6**[14] are reported for comparison.

Molecule 1		Molecule 2		**6**
Fe(1)–Fe(2)	2.5218(7)	Fe(3)–Fe(4)	2.5267(8)	2.5595(4)
Fe(1)–C(11)	1.736(4)	Fe(3)–C(41)	1.743(5)	1.745(2)
Fe(1)–C(12)	1.908(4)	Fe(3)–C(42)	1.910(4)	1.9537(19)
Fe(2)–C(12)	1.885(4)	Fe(4)–C(42)	1.897(4)	1.8702(18)
Fe(1)–C(15)	1.981(4)	Fe(3)–C(45)	1.972(4)	2.0032(17)
Fe(2)–C(15)	2.026(4)	Fe(4)–C(45)	2.016(4)	2.0648(17)
Fe(2)–C(14)	2.068(4)	Fe(4)–C(44)	2.067(4)	2.045(17)
Fe(2)–C(13)	1.939(4)	Fe(4)–C(43)	1.941(4)	1.9647(17)
C(11)–O(11)	1.152(4)	C(41)–O(41)	1.146(4)	1.153(2)
C(12)–O(12)	1.186(4)	C(42)–O(42)	1.177(4)	1.182(2)
C(14)–C(13)	1.409(5)	C(44)–C(43)	1.399(5)	1.407(2)
C(15)–C(14)	1.422(5)	C(45)–C(44)	1.424(5)	1.431(2)
C(15)–N(1)	1.419(4)	C(45)–N(2)	1.441(4)	1.395(2)
C(14)–S(1)	1.795(4)	C(44)–S(2)	1.796(4)	
C(13)–C(16)	1.317(5)	C(43)–C(46)	1.312(5)	1.317(3)
S(1)–C(25)	1.764(4)	S(2)–C(55)	1.762(4)	
N(1)–C(15)–C(14)	114.7(3)	C(44)–C(45)–N(2)	114.4(3)	
C(14)–C(15)–Fe(1)	119.7(3)	C(44)–C(45)–Fe(3)	120.3(3)	117.16(2)
C(13)–C(14)–C(15)	117.5(3)	C(43)–C(44)–C(45)	117.7(3)	120.66(16)
C(13)–C(14)–S(1)	122.4(3)	C(43)–C(44)–S(2)	122.2(3)	
C(15)–C(14)–S(1)	117.2(3)	C(45)–C(44)–S(2)	117.3(3)	
C(16)–C(13)–C(14)	143.5(4)	C(46)–C(43)–C(44)	143.5(4)	141.06(18)
C(18)–N(1)–C(15)	119.4(3)	C(48)–N(2)–C(45)	118.4(3)	120.83(14)
C(18)–N(1)–C(17)	118.3(3)	C(48)–N(2)–C(47)	118.3(3)	115.04(15)
C(15)–N(1)–C(17)	120.6(3)	C(45)–N(2)–C(47)	119.2(3)	123.88(15)
C(25)–S(1)–C(14)	101.34(17)	C(55)–S(2)–C(44)	102.40(17)	

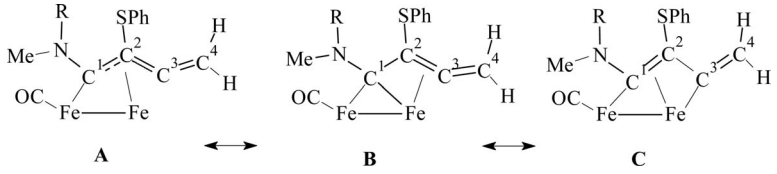

Scheme 7.

In agreement with the allyl-like coordination in **A**, Fe(2) [Fe(4) in the second independent molecule] is bonded to all three C(13), C(14), and C(15) carbon atoms [C(43), C(44), and C(45)] in the second molecule; these carbon atoms are labeled C^3, C^2, and C^1 in the schemes and both C(15)–C(14) (C^1–C^2) [1.422(5) Å; C(45)–C(44) 1.424(5) Å] and C(14)–C(13) (C^2–C^3) [1.409(5) Å; C(44)–C(43) 1.399(5) Å] bonds display some π character. At the same time, the Fe(2)–C(13) (Fe–C^3) bond length [1.939(4) Å; Fe(4)–C(43) 1.941(4) Å] is considerably shorter than those of Fe(2)–C(15) (Fe–C^1) [2.026(5) Å; Fe(4)–C(45) 2.016(4) Å] and Fe(2)–C(14) (Fe–C^2) [2.068(4) Å; Fe(4)–C(44) 2.067(4) Å], which are almost equal, suggesting an important contribution from 1-amino-1,3-butadienylidene form **C**. Finally, the fact that the C(14)–C(13) (C^2–C^3) distance [1.409(5) Å; C(44)–C(43) 1.399(5) Å] is shorter than the C(15)–C(14) (C^2–C^1) distance [1.422(5) Å; C(45)–C(44) 1.424(5) Å] indicates that aminoallenylalkylidene form **B** must also be considered. In agreement with all of the three structures **A**–**C**, the C(13)–C(16) interaction [1.317(5) Å; C(43)–C(46)b 1.312(5) Å] is almost a pure double bond, whereas the C(15)–N(1) bond [1.419(4) Å; C(45)–N(2) 1.441(4) Å] is quite elongated, which suggests limited π interaction.

A further remark concerns the reversibility of the observed γ-deprotonation. Complexes **4** and **8** upon treatment with HSO_3CF_3 in CH_2Cl_2 solution are transformed, almost quantitatively, into parent vinyliminium complexes **2a** and **2c**. This observation is consistent with the strictly related transformation of diiron butadienylidene **6** into vinyliminium complexes upon protonation with HSO_3CF_3, as recently reported.[14]

Investigation on the reactivity toward NaH was extended also to diruthenium complex **2d**, which is the ruthenium counterpart of **2a**. The aim was to evidence possible effects due to the nature of the metal atom (Ru vs. Fe).[17] Like **2a** and **2c**, diruthenium complex **2d** undergoes deprotonation at the C^3-methyl group to afford an aminobutadienylidene product (Scheme 8). However, in resulting complex **9** the bridging ligand assumes a new coordination mode, which was evidenced by X-ray diffraction.

The molecular structure of **9** is represented in Figure 2, whereas the most significant bonding parameters are listed in Table 2. The molecule can be viewed as being composed of a *cis*-$[Ru_2(CO)_2(Cp)_2]$ core to which is coordinated a μ-η^2:η^2-C(N(Me)(Xyl))C(SPh)CCH_2 ligand. The latter is essentially a 1-amino-1,3-butadienylidene ligand as in **8**, but

 © 2010 Wiley-VCH Verlag GmbH & Co. KGaA, Weinheim

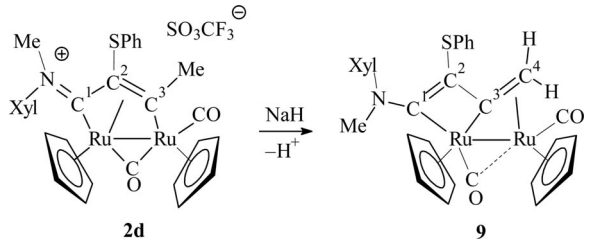

Scheme 8.

it assumes a completely different coordination mode. The bridging ligand is, in fact, coordinated in **8** to one Fe atom by C^1, whereas all three C^1, C^2, and C^3 are bonded to the second Fe atom; C^4 is not coordinated to any metal, and the bridging carbon is C^1. Conversely, in **9** the bridging ligand is π coordinated to Ru(1) by C^3 and C^4 [Ru(1)–C(13) 2.267(3) Å, Ru(1)–C(16) 2.201(3) Å] and σ coordinated to Ru(2) by C^1 and C^3 [Ru(2)–C(15) 2.073(3) Å, Ru(2)–C(13) 2.050(3) Å]; C^2 is essentially nonbonded to the metals [Ru(2)···C(14) 2.650(4) Å] and only C^3 is bonded to both Ru atoms. In agreement with the butadienylidene nature of the bridging ligand, both C(15)–C(14) [1.390(4) Å] and C(13)–C(16) [1.394(5) Å] are shorter than C(14)–C(13) [1.418(5) Å] and display strong π character.[18] Also, the C(15)–N(1) interaction [1.335(4) Å] shows some π character, and N(1) is essentially sp^2 hybridized [sum angles 360.0(16)°], as expected for an enamine group. Formally, a 1-amino-1,3-butadienylidene ligand with μ-η^2:η^2-coordination donates two electrons to each metal atom, whereas in the μ-η^1:η^3-mode displayed in **8** it donates one electron to one metal center and three to the second one. This causes a different arrangement of the CO ligands in the two complexes. In fact, there is one terminal and one bridging CO ligand in **8**, whereas they are essentially one terminal and one semibridging (strongly asymmetric) ligand in **9**. In this way, both Ru atoms formally reach 18 valence electrons. The coordination of the two CO ligands in **9** can be analyzed in more detail by the method proposed by Crabtree and Lavin[19] by considering the two angles M^1CO (denoted as θ) and CM^1M^2 (denoted as ψ). In the present case, for C(11)O(11) both θ [Ru(1)–C(11)–O(11) 174.5(3)°] and ψ [C(11)–Ru(1)–Ru(2) 101.72(11)°] completely fall in the usual range for terminal carbonyls [$\theta > 165°$, $\psi > 70°$]. Conversely, for C(12)O(12), the value of ψ [C(12)–Ru(2)–Ru(1) 64.52(11)°] agrees with a semibridging carbonyl ligand [$50° < \psi < 75°$], whereas θ [Ru(2)–C(12)–O(12) 165.1(3)°] is borderline between terminal [$\theta > 165°$] and semibridging [$145° < \theta < 165°$], suggesting a strong asymmetry in the semibridge. In agreement with this weak semibridging mode, both Ru(2)–C(12) [1.855(4) Å] and C(12)–O(12) [1.161(4) Å] are sensibly elongated compared to Ru(1)–C(11) [1.839(4) Å] and C(11)–O(11) [1.150(4) Å].

The coordination mode described above makes diruthenium complex **9** rather uncommon. The bridging aminobutadienylidene ligand in **9** shows some similarities with μ-η^2:η^3-2-butadienyl ligands in diruthenium[20] and diiron complexes[21] of type **III** (Scheme 9). Analogies can also be

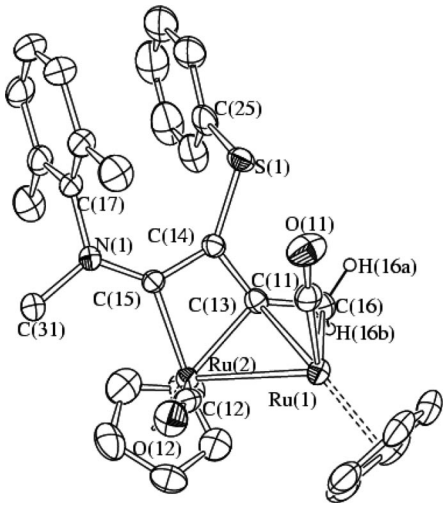

Figure 2. Molecular structure of **9** with key atoms labeled [all H atoms except for H(16a) and H(16b) are omitted for clarity]. Thermal ellipsoids are at the 30% probability level.

Table 2. Selected bond lengths [Å] and angles [°] for **9**.

Ru(2)–C(12)	1.855(4)	C(12)–O(12)	1.161(4)
Ru(2)–C(13)	2.050(3)	C(13)–C(16)	1.394(5)
Ru(2)–C(15)	2.073(3)	C(13)–C(14)	1.418(5)
Ru(2)–Ru(1)	2.8022(4)	C(14)–C(15)	1.390(4)
Ru(1)–C(11)	1.839(4)	C(14)–S(1)	1.766(3)
Ru(1)–C(16)	2.201(3)	C(15)–N(1)	1.335(4)
Ru(1)–C(13)	2.267(3)	Ru(1)···C(12)	2.612(4)
C(11)–O(11)	1.150(4)	Ru(2)···C(14)	2.650(4)
O(11)–C(11)–Ru(1)	174.5(3)	N(1)–C(15)–Ru(2)	130.9(2)
O(12)–C(12)–Ru(2)	165.1(3)	C(14)–C(15)–Ru(2)	97.9(2)
C(16)–C(13)–C(14)	134.4(3)	C(15)–N(1)–C(17)	123.9(3)
C(15)–C(14)–C(13)	100.8(3)	C(15)–N(1)–C(31)	121.4(3)
C(15)–C(14)–S(1)	134.1(3)	C(17)–N(1)–C(31)	114.7(3)
C(13)–C(14)–S(1)	124.6(2)	C(14)–S(1)–C(25)	104.76(19)
N(1)–C(15)–C(14)	131.0(3)	C(13)–C(16)–Ru(1)	74.42(19)

envisaged with the trinuclear complex [$Ru_3(CO)(\mu_3$-η^4-CH_2=CC(*i*Pr)=CH)(μ-PPh_2)(μ-H)] (**IV**)[22] (Scheme 9), in which the butadienylidene ligand is coordinated to a third metal through the terminal olefin group.

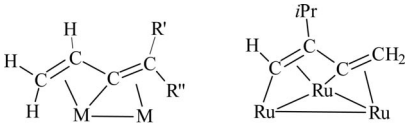

III **IV**

Scheme 9.

The spectroscopic properties of **9** are consistent with the structure found in the solid state. The IR spectrum of **9** (in CH_2Cl_2 solution) displays two νCO absorptions (1938, 1879 cm^{-1}) attributable to the terminal and bridging CO ligands, respectively. The frequency of the μ-CO band in **9** is about 100 cm^{-1} higher than that in **4** and **8**, in agreement with its semibridging character. The signals in the ^{13}C NMR spectrum that are due to the C^1–C^4 carbon atoms of the bridging frame are quite similar to those of **4** and **8**, except for the resonance attributable to the CH_2 termina-

 © 2010 Wiley-VCH Verlag GmbH & Co. KGaA, Weinheim

tion (C^4), which can be diagnostic of the different coordination in the two cases. When the $C{=}CH_2$ end of the butadienyl ligand is uncoordinated, as in **4** and **8** or in the complex $[Fe_2\{\mu\text{-}\eta^1{:}\eta^3\text{-}C(Ph)C(Ph)C{=}CH_2\}(\mu\text{-}CO)(CO)(Cp)_2]$,[13] the C^4 atom gives rise to a signal at about δ = 102–105 ppm. Conversely, in **9** the corresponding resonance is at δ = 19 ppm, which is closer to the signals found in the $\mu\text{-}\eta^2{:}\eta^3$-2-butadienyl diruthenium complex of type **III** (Scheme 9),[20] which exhibit coordination of the $C{=}CH_2$ termination.

Other relevant resonances, in the ^1H NMR spectrum, are those due to the CH_2 unit, which appear as doublets ($^2J_{H,H}$ = 2.20 Hz) at δ = 3.33 and 3.17 ppm. In the ^{13}C NMR spectrum, the resonances attributable to C^1, C^2, and C^3 are observed at δ = 173.8, 92.8, and 172.2 ppm, respectively, and are consistent with the butadienylidene nature of the bridging frame.

Finally, the study concerned the reactivity of complexes **2e** and **2f**, characterized by the presence of a CH_2OH group in place of the methyl group as the β-substituent in the bridging ligand (Scheme 10). As expected, deprotonation takes place at the hydroxy group rather than at the C^4-H, but the overall result consists of an intramolecular cyclization, as shown in Scheme 10. The reactions afford zwitterionic complexes **10a** and **10b** in good yields.

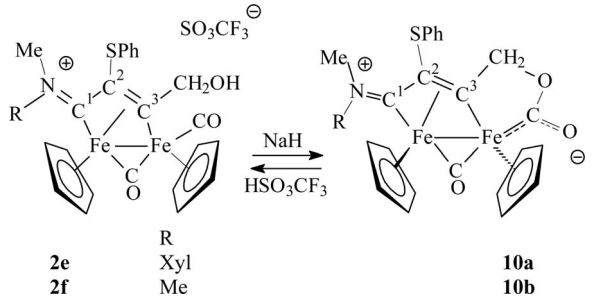

Scheme 10.

Complexes **10a** and **10b** were characterized by spectroscopy and elemental analysis. Moreover, the X ray structure of **10a** was determined: the ORTEP molecular diagram is shown in Figure 3, whereas the most relevant bond lengths and angles are reported in Table 3. The molecule can be viewed as being composed of a bridging $\mu\text{-}\eta^2{:}\eta^3$-$C\{CH_2OC(O)\}{=}C(SPh)C{=}N(Me)(Xyl)$ ligand coordinated to a *trans*-$[Fe_2(\mu\text{-}CO)(Cp)_2]$ core. As for the butadienylidene complexes discussed above, the highly delocalized nature of the π interaction within the bridging frame is better illustrated by considering different limiting resonance formulas (**D** and **E**, Scheme 11). In the first formulation (**D**), the bridging ligand is depicted as a zwitterionic vinyliminium, where C^3 is bonded through a methylene group to a terminal dialkoxocarbene ligand. The second formulation (**E**) does not require any charge separation, and the bridging ligand is essentially a vinylaminocarbene bonded to Fe(2) through a terminal aminocarbene and the π system of the vinyl group, whereas it is σ bonded to Fe(1) atom and there is also a σ-C-bonded carboxylate group coordinated to the same iron center. In this case, the CO ligand must be considered bound only to Fe(1) in order that each iron center could reach an exact electron count. In keeping with this two formulations, both Fe(2)–C(15) [1.832(3) Å] and C(15)–N(1) [1.321(4) Å] display π character and both Fe(2)–C(14) [2.054(3) Å] and Fe(2)–C(13) [1.986(3) Å] are in agreement with a π-bonded vinyl group. Even though C(13)–C(14) [1.411(4) Å] is slightly shorter than C(14)–C(15) [1.427(4) Å] (as expected for both **D** and **E**), they both display some π character, whereas C(13)–C(16) [1.501(5) Å], C(16)–O(1) [1.429(4) Å], and O(1)–C(12) [1.396(4) Å] are almost pure single bonds [even though the latter is sensibly shorter, probably because of the vicinity of the sp^2 C(12) carbon]. The C(12)–O(12) interaction [1.205(4) Å] is very

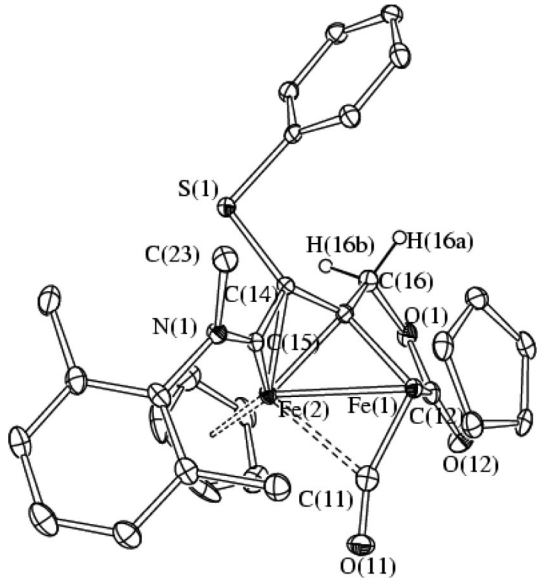

Figure 3. Molecular structure of **10a**·0.33CH_2Cl_2 with key atoms labeled [all H atoms except for H(16a) and H(16b) are omitted for clarity]. Thermal ellipsoids are at the 30% probability level.

Table 3. Selected bond lengths [Å] and angles [°] for **10a**·0.33CH_2Cl_2.

C(11)–O(11)	1.165(4)	C(14)–Fe(2)	2.054(3)
C(11)–Fe(1)	1.777(4)	C(15)–N(1)	1.321(4)
C(11)–Fe(2)	2.336(3)	C(15)–Fe(2)	1.832(3)
C(13)–C(14)	1.411(4)	C(16)–O(1)	1.429(4)
C(13)–C(16)	1.501(5)	O(1)–C(12)	1.396(4)
C(13)–Fe(1)	1.905(3)	C(12)–O(12)	1.205(4)
C(13)–Fe(2)	1.986(3)	C(12)–Fe(1)	1.942(3)
C(14)–C(15)	1.427(4)	C(23)–N(1)	1.480(4)
C(14)–S(1)	1.798(3)	Fe(1)–Fe(2)	2.6216(7)
O(11)–C(11)–Fe(1)	156.9(3)	O(1)–C(16)–C(13)	107.7(3)
O(11)–C(11)–Fe(2)	124.9(3)	C(12)–O(1)–C(16)	113.4(2)
Fe(1)–C(11)–Fe(2)	77.88(13)	O(12)–C(12)–O(1)	115.3(3)
C(14)–C(13)–C(16)	125.7(3)	O(12)–C(12)–Fe(1)	128.4(3)
C(13)–C(14)–C(15)	113.2(3)	O(1)–C(12)–Fe(1)	116.3(2)
C(13)–C(14)–S(1)	124.2(2)	C(15)–N(1)–C(24)	118.2(3)
C(15)–C(14)–S(1)	118.3(2)	C(15)–N(1)–C(23)	123.2(3)
N(1)–C(15)–C(14)	129.9(3)	C(24)–N(1)–C(23)	118.6(3)
N(1)–C(15)–Fe(2)	148.9(3)	C(17)–S(1)–C(14)	101.56(15)
C(14)–C(15)–Fe(2)	77.03(19)		

 © 2010 Wiley-VCH Verlag GmbH & Co. KGaA, Weinheim

short and would suggest a double bond in agreement with **E**, but at the same time Fe(1)–C(12) [1.942(3) Å] is shorter than a pure Fe–C(sp^2) σ interaction, indicating the presence of some double bond interaction, as expected for zwitterionic form **D**. Typical values for a pure Fe–C(sp^2) single bond are, for instance, 1.971(3) Å in [Fe(Cp)(CO)$_2$-(CH=CHCH=CHBr)][23] and 1.956(7) Å in the vinyl complex [Fe$_2${μ-CN(Me)(Xyl)}(m-CO)(CO){C(OMe)=CHC-(=NPh)(Tol)}(Cp)$_2$].[24] The CO ligand present within the complex can be considered as semibridging on the basis of the θ [Fe(1)–C(11)–O(11) 156.9(3)°] and ψ [C(11)–Fe(1)–Fe(2) 60.61(11)°] angles previously defined.[19] In agreement with this, Fe(1)–C(11) [1.777(4) Å] is considerably shorter than Fe(2)–C(11) [2.336(3) Å].

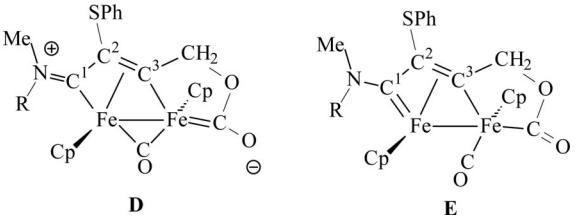

Scheme 11.

The IR spectra (in CH_2Cl_2 solutions) exhibit three intense bands (e.g., for **10a** at 1870, 1643, and 1553 cm^{-1}) attributed to the bridging carbonyl, the acyl, and the $C_\alpha N$ interaction, respectively. The NMR spectra evidence the presence in solution of single isomeric forms. NOE investigations carried out on **10a** have outlined that the iminium substituents adopt a *Z* configuration, and the Cp ligands adopt a mutual *trans* geometry, coherently with that found in the solid state. In the ^{13}C NMR spectra, the resonances due to C^1, C^2, and C^3 are observed at ca. δ = 230, 60, and 210 ppm, respectively, which are values typical for a μ-vinyliminium ligand.[2] Moreover, the bridging CO is found at ca. δ = 235 ppm, whereas the acyl carbon atom resonates at δ = 220 ppm.

The synthesis of **10a** and **10b** is clearly the result of deprotonation of the CH_2OH group in **2e** and **2f**, followed by intramolecular attack of the alkoxide to a CO ligand. The transformation is accompanied by *cis–trans* isomerization (referred to the mutual Cp position with respect to the Fe–Fe bond), which is likely the consequence of steric effects.

The formation of **10a** and **10b** is reversible, and parent complexes **2e** and **2f** can be reformed, respectively, upon treatment of **10a** and **10b** in CH_2Cl_2 solution with one equivalent of HSO_3CF_3. Interestingly, the reverse protonation reaction of **2e** and **2f** starting from **10a** and **10b**, also implies the reverse *trans* to *cis* isomerization of the Cp ligands.

Conclusions

Diiron and diruthenium vinyliminium complexes containing a –SPh group in the α position are reactive toward NaH. They can undergo fragmentation, affording five-membered metallacycles, but the most relevant result is the observed γ-deprotonation, which transforms the bridging frame into a butadienylidene ligand. This reaction relates to the conversion of α,β-unsaturated iminium ions into the corresponding dienamines by γ-deprotonation, which is a relatively uncommon transformation. In our case, because the conversion involves α,β-unsaturated iminium species acting as bridging ligands, the metal centers provide stability to the resulting dienamine fragment, which is better described as a butadienylidene ligand. An interesting aspect is the different coordination mode that the same butadienylidene ligand assumes in the diiron and diruthenium complexes **4** and **9**, respectively (Scheme 12).

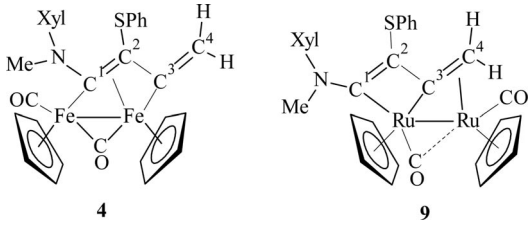

Scheme 12.

This result evidences the high flexibility of dinuclear complexes, in that they can rearrange ancillary ligands and accommodate bridging frames in different ways to provide maximum stability. As a consequence, it is possible to observe molecular species otherwise difficult to obtain and that are potentially able to provide new reaction modes.

Experimental Section

General Data: All reactions were routinely carried out under a nitrogen atmosphere by using standard Schlenk techniques. Solvents were distilled immediately before use under a nitrogen atmosphere from appropriate drying agents. Chromatography separations were carried out on columns of deactivated alumina (4% w/w water). Glassware was oven-dried before use. Infrared spectra were recorded at 298 K with a Perkin–Elmer Spectrum 2000 FTIR spectrophotometer, and elemental analyses were performed with a ThermoQuest Flash 1112 Series EA Instrument. MS (ESI) spectra were recorded with Waters Micromass ZQ 4000 with samples dissolved in CH_3CN. All NMR measurements were recorded at 298 K with Mercury Plus 400 instrument. The chemical shifts for ^1H and ^{13}C were referenced to internal TMS. The spectra were fully assigned by DEPT experiments and ^1H–^{13}C correlation through gs-HSQC and gs-HMBC experiments.[25] NOE measurements were recorded by using the DPFGSE-NOE sequence.[26] All reagents were commercial products (Aldrich) of the highest purity available and used as received. Complexes **2a**–**f** were prepared by literature methods.[12]

[Fe(CO)(Cp){C^{1}N(Xyl)(Me)C^2(SPh)C^3(Me)C(O)}] (3) and [Fe$_2${μ-η^1:η^3-C^{1}N(Xyl)(Me)=C^2(SPh)C^3=CH$_2$}(μ-CO)(CO)(Cp)$_2$] (4)

Method 1: A solution of **2a** (200 mg, 0.270 mmol) in thf (10 mL) was treated with NaH (40 mg, 1.67 mmol). The resulting mixture was stirred for 120 min, and it was then filtered through a Celite pad. Removal of the solvent gave a residue that was chromatographed on alumina (CH_2Cl_2). The first fraction afforded, upon removal of the solvent, a brown solid, corresponding to **4**. A second green-brown fraction was collected, yielding **3**. Data for **4**: Yield:

 © 2010 Wiley-VCH Verlag GmbH & Co. KGaA, Weinheim

32 mg, 20%. $C_{31}H_{29}Fe_2NO_2S$ (591.32): calcd. C 62.97, H 4.94, N 2.37; found C 63.09, H 4.81, N 2.50. IR (CH_2Cl_2): $\tilde{\nu}$ = 1960 (vs, νCO), 1776 (s, νCO) cm^{-1}. ^1H NMR (400 MHz, $CDCl_3$): δ = 7.54–7.01 (8 H, $Me_2C_6H_3$ and SPh); 4.75, 4.56 (br., 2 H, CH_2); 4.69, 4.38 (s, 10 H, Cp); 3.83 (s, 3 H, NMe); 2.74, 2.19 (s, 6 H, $Me_2C_6H_3$) ppm. ^{13}C NMR (100 MHz, $CDCl_3$): δ = 266.3 (μ-CO); 215.1 (CO); 200.3 (C^1); 178.3 (C^3); 139.5–126.4 ($Me_2C_6H_3$ and SPh); 102.4 (CH_2); 87.7, 85.1 (Cp); 82.2 (C^2); 48.9 (NMe); 20.1, 18.9 ($Me_2C_6H_3$) ppm. Data for **3**: Yield: 83 mg, 65%. $C_{26}H_{25}FeNO_2S$ (471.39): calcd. C 66.25, H 5.35, N 2.97; found C 66.33, H 5.41, N 2.89. IR (CH_2Cl_2): $\tilde{\nu}$ 1916 (vs, νCO), 1598 (m, νCO) cm^{-1}. ^1H NMR (400 MHz, $CDCl_3$): δ = 7.54–7.01 (8 H, $Me_2C_6H_3$ and SPh); 4.62 (s, 5 H, Cp); 3.81 (s, 3 H, NMe); 2.26, 2.09 (s, 6 H, $Me_2C_6H_3$); 1.70 (s, 3 H, C^3Me) ppm. ^{13}C NMR (100 MHz, $CDCl_3$): δ = 266.5 (C=O); 255.0 (C^1); 223.4 (CO); 169.7 (C^3); 158.0 (C^2); 139.5–126.4 ($Me_2C_6H_3$ and SPh); 86.3 (Cp); 51.4 (NMe); 18.5, 17.9 ($Me_2C_6H_3$); 13.0 (C^3Me) ppm.

Method 2: Compound **2a** (150 mg, 0.20 mmol) in thf (10 mL) was cooled to –50 °C and treated with a thf solution (4 mL) of $NaC_{10}H_8$ (0.15 M), freshly prepared from Na and naphthalene. The mixture was warmed to room temperature, stirred for an additional 60 min, and filtered through a Celite pad. Removal of the solvent and chromatography on alumina (CH_2Cl_2) gave a brown band of **3**. Yield: 84 mg, 87%.

Method 3: Compound **2a** (150 mg, 0.20 mmol) in thf (10 mL) was treated with *t*BuOK (112 mg, 1.0 mmol). The reaction mixture was stirred at room temperature for 2 h, and it was then filtered through a Celite pad. Solvent removal and chromatography of the residue on alumina (CH_2Cl_2) gave **4**. Yield: 85 mg, 71%.

[Fe(CO)(Cp){C^1N(Me)$_2C^2$(SPh)C^3(Me)C(O)}] (7): Prepared by a procedure similar to that described for **3** (method 1) by treating **2b** (176 mg, 0.324 mmol) in thf (10 mL) with NaH (39 mg, 1.63 mmol). Yield: 105 mg, 85%. $C_{19}H_{19}FeNO_2S$ (381.27): calcd. C 59.85, H 5.02, N 3.67; found C 59.92, H 4.95, N 3.60. IR (CH_2Cl_2): $\tilde{\nu}$ 1922 (vs, νCO), 1582 (m, νCO) cm^{-1}. ^1H NMR (400 MHz, $CDCl_3$): δ = 7.50–6.97 (5 H, Ph); 4.52 (s, 5 H, Cp); 3.66, 3.47 (s, 6 H, NMe); 1.73 (s, 3 H, C^3Me) ppm. ^{13}C NMR (100 MHz, $CDCl_3$): δ = 271.8 (C^1); 267.9 (CO_{acyl}); 221.3 (CO); 168.1 (C^3); 157.5 (C^2); 146.6 ($C_{ipso\text{-}Ph}$); 133.2–123.7 (Ph); 84.6 (Cp); 52.8, 46.6 (NMe); 12.9 (C^3Me) ppm.

[Fe_2{μ-η^1:η^3-C^1N(C_6H_4OMe)(Me)=C^2(SPh)C^3=CH_2}(μ-CO)(CO)-(Cp)$_2$] (8): Prepared by a procedure similar to that described for **4** (method 1) by treating **2c** (160 mg, 0.215 mmol) with NaH (45 mg, 1.88 mmol). Crystals of **8** suitable for X-ray analysis were obtained from a CH_2Cl_2 solution layered with *n*-pentane at –20 °C. Yield: 103 mg, 81%. $C_{30}H_{27}Fe_2NO_3S$ (593.30): calcd. C 60.73, H 4.59, N 2.36; found C 60.78, H 4.64, N 2.44. IR (CH_2Cl_2): $\tilde{\nu}$ 1961 (vs, νCO), 1773 (s, νCO) cm^{-1}. ^1H NMR (400 MHz, $CDCl_3$): δ = 7.12–6.91 (9 H, Ph and C_6H_4OMe); 4.92, 4.46 (d, $^2J_{H,H}$ = 2.93 Hz, CH_2); 4.83, 4.74 (s, 10 H, Cp); 4.16 (s, 3 H, NMe); 3.79 (s, 3 H, OMe) ppm. ^{13}C NMR (100 MHz, $CDCl_3$): δ = 267.5 (μ-CO); 213.9 (CO); 196.4 (C^1); 169.9 (C^3); 152.0–114.1 (C_6H_4Me); 105.6 (CH_2); 86.8, 86.2 (Cp); 79.6 (C^2); 55.3 (OMe); 44.6 (NMe) ppm. MS (ESI+): *m*/*z* = 594 $[M]^+$.

[Ru_2{μ-η^2:η^3-C^1N(Me)(Xyl)=C^2(SPh)C^3=CH_2}(CO)$_2$(Cp)$_2$] (9): Prepared by a procedure similar to that described for **4** (method 1) by treating **2d** (120 mg, 0.144 mmol) with NaH (40 mg, 1.67 mmol). Yield: 74 mg, 75%. Pink crystals suitable for X-ray analysis were obtained from a CH_2Cl_2 solution layered with *n*-pentane at –20 °C. $C_{31}H_{29}NO_2Ru_2S$ (681.77): calcd. C 54.61, H 4.29, N 2.05; found C 54.64, H 4.38, N 2.00. IR (CH_2Cl_2): $\tilde{\nu}$ 1938 (vs, νCO), 1879 (m, νCO) cm^{-1}. ^1H NMR (400 MHz, $CDCl_3$): δ = 7.64–6.60 (8 H, Ph and $Me_2C_6H_3$); 5.08, 5.07 (s, 10 H, Cp); 3.48 (s, 3 H, NMe); 3.33, 3.17 (d, $^2J_{H,H}$ = 2.20 Hz, 2 H, CH_2); 2.17, 1.70 (s, 6 H, $Me_2C_6H_3$) ppm. ^{13}C NMR (100 MHz, $CDCl_3$): δ = 215.8, 200.4 (CO); 173.8 (C^1); 172.2 (C^3); 143.8 ($C_{ipso\text{-}Ph}$); 143.2 ($C_{ipso\text{-}Xyl}$); 136.8–123.0 (C_{arom}); 92.8 (C^2); 86.4, 83.4 (Cp); 46.4 (NMe); 18.7 (CH_2); 17.4, 17.2 ($Me_2C_6H_3$) ppm. MS (ESI): *m*/*z* (%) = 683 (20) $[M]^+$, 574 (100) $[M – SPh]^+$, 546 (22) $[M – SPh – CO]^+$.

[Fe_2{μ-η^1:η^3-C^3{CH_2OC(O)}=C^2(SPh)C^1=N(Me)(R)}(μ-CO)(Cp)$_2$] (R = Xyl, 10a): A solution of **2e** (90 mg, 0.119 mmol) in thf (10 mL) was treated with NaH (25 mg, 1.04 mmol). The mixture was stirred for 2 h, and it was then filtered through an alumina pad. Solvent removal under reduced pressure gave **10a** as green microcrystalline solid. Crystals suitable for X-ray diffraction were collected from a CH_2Cl_2 solution layered with *n*-pentane at –20 °C. Yield: 61 mg, 85%. $C_{31}H_{29}Fe_2NO_3S$ (607.32): calcd. C 61.31, H 4.81, N 2.31; found C 61.36, H 4.77, N 2.22. IR (CH_2Cl_2): $\tilde{\nu}$ 1870 (s, νCO), 1643 (vs, νCO) cm^{-1}. ^1H NMR (400 MHz, $CDCl_3$): δ = 7.62–7.29 (8 H, Ph and $Me_2C_6H_3$); 5.42, 5.04 (d, $^2J_{H,H}$ = 14 Hz, 2 H, CH_2); 4.37, 4.06 (s, 10 H, Cp); 3.56 (s, 3 H, NMe); 2.61, 1.96 (s, 6 H, $Me_2C_6H_3$) ppm. ^{13}C NMR (100 MHz, $CDCl_3$): δ = 235.5 (μ-CO); 233.0 (C^1); 220.0 (OCO); 209.3 (C^3); 144.0 ($C_{ipso\text{-}Xyl}$); 137.0 ($C_{ipso\text{-}Ph}$); 134.3–126.6 (C_{arom}); 86.2, 84.6 (Cp); 64.7 (CH_2); 64.7 (C^2); 47.0 (NMe); 18.1, 17.9 ($Me_2C_6H_3$) ppm.

[Fe_2{μ-η^1:η^3-C^3{CH_2OC(O)}=C^2(SPh)C^1=N(Me)(R)}(μ-CO)(Cp)$_2$] (R = Me, 10b): Prepared by a procedure similar to that described for **10a** by treating **2f** (140 mg, 0.226 mmol) with NaH (40 mg, 1.67 mmol). Yield: 103 mg, 88%. $C_{24}H_{23}Fe_2NO_3S$ (517.20): calcd. C 55.73, H 4.48, N 2.71; found C 55.81, H 4.36, N 2.74. IR (CH_2Cl_2): $\tilde{\nu}$ 1851 (s, νCO), 1638 (vs, νCO) cm^{-1}. ^1H NMR (400 MHz, $CDCl_3$): δ = 7.85–7.16 (5 H, Ph); 5.27, 5.13 (d, $^2J_{H,H}$ = 14 Hz, 2 H, CH_2); 4.36, 4.18 (s, 10 H, Cp); 3.69, 3.19 (s, 6 H, NMe) ppm. ^{13}C NMR (100 MHz, $CDCl_3$): δ = 239.8 (μ-CO); 227.3 (C^1); 220.9 (OCO); 206.9 (C^3); 137.6 ($C_{ipso\text{-}Ph}$); 129.4, 127.7, 126.2 (C_{arom}); 86.3, 84.5 (Cp); 76.7 (CH_2); 60.5 (C^2); 46.8, 45.6 (NMe) ppm.

X-ray Crystallography: Crystal data and collection details for **8**, **9** and **10a**·0.33CH_2Cl_2 are reported in Table 4. The diffraction experiments were carried out with a Bruker APEX II (for **8** and **9**) and with a Bruker AXS SMART 2000 (for **10a**·0.33CH_2Cl_2) diffractometer equipped with a CCD detector by using Mo-K_α radiation. Data were corrected for Lorentz polarization and absorption effects (empirical absorption correction SADABS).[27] Structures were solved by direct methods and refined by full-matrix least-squares based on all data by using F^2.[28] Hydrogen atoms were fixed at calculated positions and refined by a riding model. Two independent molecules are present within the unit cell of **8**, with the same connectivity and similar bond lengths and angles. *U* restraints were applied to the C atoms in **8** (s.u. 0.01) and **9** (s.u. 0.005). Finally, the CH_2Cl_2 molecule in **10a**·0.33CH_2Cl_2 located close to a 3-axis, is disordered over six positions, three by three related by symmetry. Only the two independent images were refined isotropically by using similar distance and similar *U* restraints as well as fixed distances (SAME, SIMU, and DFIX 1.78 for all C–Cl bonds in SHELXL) and one occupancy factor per disordered group (to each atom of the first image was attributed an occupancy factor of 20.33333, and –20.33333 to the second one). CCDC-765745 (for **8**), -765746 (for **10a**·0.33CH_2Cl_2), and -765747 (for **9**) contain the supplementary crystallographic data for this paper. These data can be obtained free of charge from The Cambridge Crystallographic Data Centre via www.ccdc.cam.ac.uk/data_request/cif.

 © 2010 Wiley-VCH Verlag GmbH & Co. KGaA, Weinheim

Table 4. Crystal data and experimental details for **8**, **9**, and **10a**·0.33CH_2Cl_2.

Complex	**8**	**9**	**10a**·0.33CH_2Cl_2[a]
Formula	$C_{30}H_{27}Fe_2NO_3S$	$C_{31}H_{29}NO_2Ru_2S$	$C_{31.33}H_{29.67}Cl_{0.67}Fe_2NO_3S$
Fw	593.29	681.75	635.62
T [K]	295(2)	295(2)	100(2)
λ [Å]	0.71073	0.71073	0.71073
Crystal system	monoclinic	monoclinic	trigonal
Space group	$P2_1/n$	$P2_1/c$	$R3c$
a [Å]	9.4967(5)	12.5485(4)	30.610(4)
b [Å]	43.136(2)	13.4647(5)	30.610(4)
c [Å]	13.1154(7)	16.7588(6)	15.472(3)
α [°]	90	90	90
β [°]	92.1480(10)	102.0540(10)	90
γ [°]	90	90	120
Cell volume [Å^3]	5369.0(5)	2769.16(17)	12555(4)
Z	8	4	18
$D_{calcd.}$ [g cm^{-3}]	1.468	1.635	1.513
μ [mm^{-1}]	1.191	1.195	1.213
F(000)	2488	1368	5904
Crystal size [mm]	0.23 × 0.19 × 0.14	0.24 × 0.20 × 0.15	0.31 × 0.27 × 0.19
θ limits [°]	1.62–25.00	1.66–28.00	1.33–25.02
Reflections collected	38667	31597	35839
Independent reflections	9450 [R_{int} = 0.0603]	6600 [R_{int} = 0.0385]	4904 [R_{int} = 0.0705]
Data/restraints/parameters	9450/300/671	6600/162/337	4904/15/371
Goodness on fit on F^2	1.001	1.026	1.056
R_1 [$I > 2\sigma(I)$]	0.0444	0.0329	0.0332
wR_2 (all data)	0.0969	0.0783	0.0769
Largest diff. peak and hole [e Å^{-3}]	0.297/–0.291	0.766/–0.604	0.388/–0.224

[a] Absolute structure factor 0.013(14).

Acknowledgments

We thank the Ministero dell'Università e della Ricerca Scientifica e Tecnologica (MIUR) and the University of Bologna for financial support.

[1] a) V. Ritleng, M. J. Chetcuti, *Chem. Rev.* **2007**, *107*, 797–858; b) M. Cowie, *Can. J. Chem.* **2005**, *83*, 1043–1055; c) S. A. R. Knox, *J. Organomet. Chem.* **1990**, *400*, 255–272; d) P. Braunstein, J. Rosè, *Metal Cluster in Chemistry* (Eds.: P. Braunstein, L. A. Oro, P. R. Raithby), Wiley-VCH, Weinheim, **1999**; e) L. Busetto, P. Maitlis, V. Zanotti, *Coord. Chem. Rev.* **2010**, *254*, 470–486.

[2] a) V. G. Albano, L. Busetto, F. Marchetti, M. Monari, S. Zacchini, V. Zanotti, *Organometallics* **2003**, *22*, 1326–1331; b) V. G. Albano, L. Busetto, F. Marchetti, M. Monari, S. Zacchini, V. Zanotti, *J. Organomet. Chem.* **2004**, *689*, 528–538.

[3] a) A. Erkkilä, I. Majander, P. M. Pihko, *Chem. Rev.* **2007**, *107*, 5416–5470; b) M. Shimizu, I. Hachiya, I. Mizota, *Chem. Commun.* **2009**, *8*, 874–889.

[4] a) V. G. Albano, L. Busetto, F. Marchetti, M. Monari, S. Zacchini, V. Zanotti, *Organometallics* **2004**, *23*, 3348–3354; b) V. G. Albano, L. Busetto, F. Marchetti, M. Monari, S. Zacchini, V. Zanotti, *J. Organomet. Chem.* **2006**, *691*, 4234–4243; c) L. Busetto, F. Marchetti, S. Zacchini, V. Zanotti, *Eur. J. Inorg. Chem.* **2007**, 1799–1807.

[5] Z. Rappoport (Ed.), *The Chemistry of Enamines*, Wiley, New York, **1994**.

[6] a) S. Mukherjee, J. W. Yang, S. Hoffmann, B. List, *Chem. Rev.* **2007**, *107*, 5471–5569; b) B. List, *Acc. Chem. Res.* **2004**, *37*, 548–557; c) B. List, R. A. Lerner, C. F. Barbas III, *J. Am. Chem. Soc.* **2000**, *122*, 2395–2396.

[7] Selected reviews include: a) B. Simmons, A. M. Walji, D. W. C. MacMillan, *Angew. Chem. Int. Ed.* **2009**, *48*, 4349–4353; b) D. Enders, C. Grondal, M. R. M. Hüttl, *Angew. Chem. Int. Ed.* **2007**, *46*, 1570–1581; c) P. Melchiorre, M. Marigo, A. Carlone, G. Bartoli, *Angew. Chem. Int. Ed.* **2008**, *47*, 6138–6171; d) B. List, *Chem. Commun.* **2006**, *8*, 819–824.

[8] L. Busetto, F. Marchetti, S. Zacchini, V. Zanotti, *Organometallics* **2005**, *24*, 2297–2306.

[9] L. Busetto, F. Marchetti, S. Zacchini, V. Zanotti, *Organometallics* **2006**, *25*, 4808–4816.

[10] L. Busetto, F. Marchetti, S. Zacchini, V. Zanotti, *Organometallics* **2007**, *26*, 3577–3584.

[11] L. Busetto, F. Marchetti, S. Zacchini, V. Zanotti, *Organometallics* **2008**, *27*, 5058–5066.

[12] L. Busetto, F. Marchetti, R. Mazzoni, M. Salmi, S. Zacchini, V. Zanotti, *J. Organomet. Chem.* **2008**, *693*, 3191–3196.

[13] C. P. Casey, W. H. Miles, P. J. Fagan, K. J. Haller, *Organometallics* **1985**, *4*, 559–563.

[14] L. Busetto, F. Marchetti, M. Salmi, S. Zacchini, V. Zanotti, *Eur. J. Inorg. Chem.* **2008**, 2437–2447.

[15] S. Bertelsen, M. Marigo, S. Brandes, P. Diner, K. A. Jørgensen, *J. Am. Chem. Soc.* **2006**, *128*, 12973.

[16] a) B. Han, Z.-Q. He, J.-L. Li, R. Li, K. Jiang, T.-Y. Liu, Y.-C. Chen, *Angew. Chem. Int. Ed.* **2009**, *48*, 5474 –5477; b) B.-C. Hong, M.-F. Wu, H.-C. Tseng, G.-F. Huang, C.-F. Su, J.-H. Liao, *J. Org. Chem.* **2007**, *72*, 8459; c) B.-C. Hong, H.-C. Tseng, S.-H. Chen, *Tetrahedron* **2007**, *63*, 2840; d) R. M. de Figueiredo, R. Fröhlich, M. Christmann, *Angew. Chem. Int. Ed.* **2008**, *47*, 1450–1453.

[17] L. Busetto, F. Marchetti, S. Zacchini, V. Zanotti, *J. Organomet. Chem.* **2006**, *691*, 2424.

[18] F. H. Allen, O. Kennard, D. G. Watson, L. Brammer, A. G. Orpen, R. Taylor, *J. Chem. Soc. Perkin Trans. 2* **1987**, S1–S19.

[19] R. H. Crabtree, M. Lavin, *Inorg. Chem.* **1986**, *25*, 805–812.

[20] J. N. L. Dennett, S. A. R. Knox, J. P. H. Charmant, A. L. Gillon, A. G. Orpen, *Inorg. Chim. Acta* **2003**, *354*, 29–40.

[21] S. M. Breckenridge, S. A. MacLaughlin, N. J. Taylor, A. J. Carty, *J. Chem. Soc., Chem. Commun.* **1991**, 1718–1720.

[22] a) D. Nucciarone, N. J. Taylor, A. J. Carty, *Organometallics* **1984**, *3*, 177–179; b) D. Nucciarone, N. J. Taylor, A. J. Carty,

 © 2010 Wiley-VCH Verlag GmbH & Co. KGaA, Weinheim

A. Tiripicchio, M. Tiripicchio, C. E. Sappa, *Organometallics* **1988**, *7*, 118–126.
[23] R. Ferede, M. Noble, A. W. Cordes, N. T. Allison, J. Lay, *J. Organomet. Chem.* **1988**, *649*, 64–69.
[24] L. Busetto, F. Marchetti, S. Zacchini, V. Zanotti, *Inorg. Chim. Acta* **2005**, *358*, 1469–1484.
[25] W. Wilker, D. Leibfritz, R. Kerssebaum, W. Beimel, *Magn. Reson. Chem.* **1993**, *31*, 287–292.
[26] K. Stott, J. Stonehouse, J. Keeler, T. L. Hwang, A. J. Shaka, *J. Am. Chem. Soc.* **1995**, *117*, 4199–4200.
[27] G. M. Sheldrick, *SADABS, Program for Empirical Absorption Correction*, University of Göttingen, Germany, **1996**.
[28] G. M. Sheldrick, *SHELX97, Program for Crystal Structure Determination*, University of Göttingen, Germany, **1997**.

Received: March 3, 2010
Published Online: May 11, 2010

 © 2010 Wiley-VCH Verlag GmbH & Co. KGaA, Weinheim